

Highly asymmetric magnetic behavior in exchange biased systems induced by noncollinear field cooling

E. Jiménez,¹ J. Camarero,^{1,2,a)} J. Sort,³ J. Nogués,⁴ A. Hoffmann,⁵ F. J. Teran,² P. Perna,² J. M. García-Martín,⁶ B. Dieny,⁷ and R. Miranda^{1,2}

¹Departamento de Física de la Materia Condensada and Instituto "Nicolás Cabrera," Universidad Autónoma de Madrid, 28049 Madrid, Spain

²Instituto Madrileño de Estudios Avanzados en Nanociencia IMDEA-Nanociencia, Campus Universidad Autónoma de Madrid, 28049 Madrid, Spain

³Institució Catalana de Recerca i Estudis Avançats (ICREA) and Departament de Física, Universitat Autònoma de Barcelona, 08193 Bellaterra, Spain

⁴Institució Catalana de Recerca i Estudis Avançats (ICREA) and Centre d'Investigació en Nanociència i Nanotecnologia (ICN-CSIC), Edifici CM7, Campus Universitat Autònoma de Barcelona, 08193 Bellaterra, Spain

⁵Materials Science Division and Center for Nanoscale Materials, Argonne National Laboratory, Argonne, Illinois 60439, USA

⁶Instituto de Microelectrónica de Madrid (IMM/CNM-CSIC), 28760 Tres Cantos, Spain

⁷SPINTEC, UMR 8191 CEA/CNRS/UJF, CEA/Grenoble, INAC, 38054 Grenoble Cedex 9, France

(Received 22 July 2009; accepted 3 September 2009; published online 25 September 2009)

A detailed study of the angular dependence of the magnetization reversal in polycrystalline ferromagnetic (FM)/antiferromagnetic Co/IrMn bilayers with noncollinear FM and unidirectional anisotropies shows a peculiar asymmetric magnetic behavior. The anisotropy configuration is set via a field cooling (FC) procedure with the magnetic field misaligned with respect to the easy magnetization direction of the FM layer. Different magnetization reversal modes are observed for either positive or negative angles with respect to the FC direction. The angular dependence of both coercivity and exchange bias also clearly displays the broken symmetry of the induced noncollinearity. Our findings are reproduced with a modified Stoner–Wohlfarth model including the induced anisotropy configuration. Our results highlight the importance of the relative angle between anisotropies in exchange bias systems, opening a new path for the tailoring of their magnetic properties. © 2009 American Institute of Physics. [doi:10.1063/1.3236768]

Ferromagnetic/antiferromagnetic (FM/AFM) structures¹ are at the heart of today's spintronic devices, stabilizing the direction of FM reference layers, while taking advantage of the interfacial exchange interaction effects.² The most notable consequences of the FM/AFM exchange coupling are a shift in the hysteresis loop of the FM layer, called exchange bias $\mu_0 H_E$, an enhanced coercivity $\mu_0 H_C$, and an asymmetry in the magnetization reversal process. Experiments have shown that pinned (unpinned) uncompensated AFM spins at the interface are correlated with $\mu_0 H_E$ (Ref. 3) (coercivity enhancement⁴), and that the competition between anisotropies determines the asymmetric behavior of the magnetization reversal.^{5,6}

Different intrinsic parameters (e.g., materials, anisotropies, thicknesses, and shapes)² as well as extrinsic ones [e.g., field cooling (FC) procedures^{7–10}] have been explored to understand the exchange coupling phenomena in FM/AFM systems, aiming at improving the performance of magnetic devices. In general, the interfacial exchange coupling effects depend on the strength of the anisotropies⁵ as well as their relative orientation,⁶ exhibiting a complex phase diagram of different reversal modes.^{5,6,11–15} In fact, the relative orientation between the intrinsic FM anisotropy and the induced interfacial unidirectional anisotropy can be controlled by different FC procedures, varying both strength,^{7,8} FC angle,^{6,9,10} and/or interfacial magnetic frustration.^{14,15}

In this letter we present a detailed study on the magnetization reversal of FM/AFM systems with a noncollinear uniaxial, K_U , and unidirectional, K_E , anisotropy configuration. Our work reveals the importance of taking into account the misalignment between the K_U direction and the direction of the applied field during the FC procedure in order to properly account for the asymmetry of the magnetization reversal and the angular dependences of $\mu_0 H_C$ and $\mu_0 H_E$.

The collinear and noncollinear relative orientation between the intrinsic uniaxial anisotropy of the FM, K_U , and the induced unidirectional anisotropy, K_E , is achieved after warming a sputtered polycrystalline Co(12 nm)/IrMn(4 nm) bilayer⁵ to 420 K and FC to room temperature (RT) in a 0.3 T external field either aligned (collinear, $\beta_{FC}=0^\circ$) or misaligned by an angle $\beta_{FC}=20^\circ$ (noncollinear) with respect to the easy magnetization direction of the FM layer. Angular dependent, high resolution, vectorial Kerr magnetometry measurements have been performed at RT to study the dependence of the reversal of both parallel (M_{\parallel}) and transverse (M_{\perp}) magnetization components with respect to the applied field angle α_H , where $\alpha_H=0^\circ$ is defined as the FC direction.

Figure 1 compares in-plane magnetization hysteresis loops parallel and perpendicular to the FC direction for the collinear ($\beta_{FC}=0^\circ$) and noncollinear ($\beta_{FC}=20^\circ$) coupling configurations [as depicted in Fig. 1(a)]. For $\alpha_H=0^\circ$, the top graphs of Fig. 1(b) show that both the induced exchange bias and the coercivity for both cooling angles are similar and that the magnetization behaves symmetrically whether the

^{a)}Electronic mail: julio.camarero@uam.es.

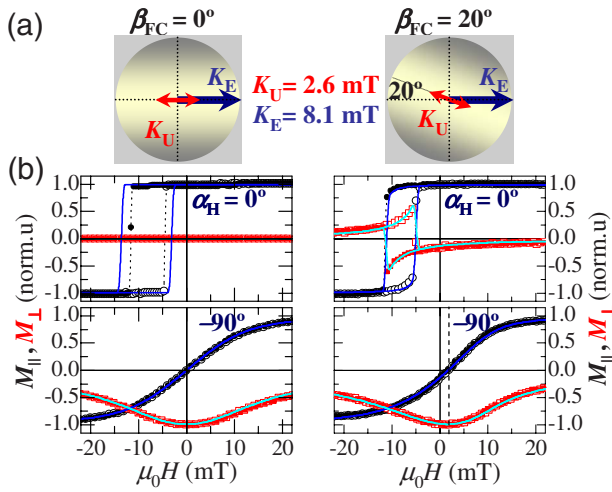


FIG. 1. (Color online) Magnetization reversal of a Co/IrMn bilayer for different FC angles β_{FC} with respect to the FM anisotropy axis. (a) Schematic representation of the anisotropy configuration after the FC procedures. The size of the arrows is scaled to the experimental values of K_U and K_E . (b) Hysteresis loops $M_{\parallel}(H)$ (circles) and $M_{\perp}(H)$ (squares) at selected field angles α_H , parallel (top panels) and perpendicular (bottom) to the FC direction. To clarify the evolution of the magnetization, the two branches of the experimental loops have been depicted with different filled symbols. The solid lines are the simulated curves obtained using the SW model with the anisotropy configurations depicted in (a).

field is swept along (increasing field branch) or against (decreasing field branch) the FC direction. However, the reversal in each system takes place in a different fashion. In both cases, M_{\parallel} reverses mainly via a sharp irreversible transition, indicating that the reversal is mainly governed by nucleation and propagation of magnetic domains. For the collinear configuration $M_{\perp}=0$ in the whole field loop, whereas for the noncollinear case a clear hysteresis with both smooth reversible and sharp irreversible transitions is observed. This indicates that during the sharp transitions the magnetization in the nucleated magnetic domains is aligned parallel to the external field for the collinear coupling configuration, while it is nonparallel for the noncollinear case. For $\alpha_H=90^\circ$, perpendicular to the FC direction, smooth reversible transitions are observed in both M_{\parallel} and M_{\perp} loops for both coupling configurations, indicating that magnetization rotation is the relevant process during reversal. Remarkably, the M_{\parallel} hysteresis loop exhibits a shift along the field axis for the noncollinear anisotropy configuration [marked with a vertical dashed line in the right bottom graph of Fig. 1(b)].

An unusual asymmetric magnetization reversal behavior is found for the noncollinear coupled FM/AFM bilayer. The right and left panels of Fig. 2 show the hysteresis loops acquired around the FC direction for negative and positive α_H values, respectively. In general, both smooth reversible and sharp irreversible transitions are observed in both components of magnetization, indicating rotation and nucleation and further propagation of magnetic domains, respectively. The asymmetric reversal behavior is found by the differently rounded M_{\parallel} transitions and different maximum values of M_{\perp} observed in the decreasing and increasing field branches of the hysteresis loop. Similar features were also observed in other collinear coupled FM/AFM systems.⁵ In contrast, several remarkable differences are found in the present study. For the noncollinear coupled bilayer, depending of the field angle, M_{\perp} can reverse in one semicircle (i.e., M_{\perp} can be

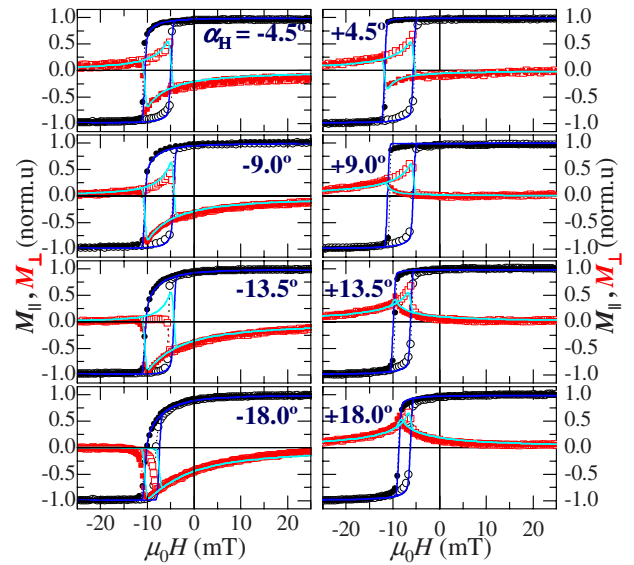


FIG. 2. (Color online) In-plane hysteresis loops, $M_{\parallel}(H)$ (circles) and $M_{\perp}(H)$ (squares), of the noncollinear coupled Co/IrMn bilayer at the labeled field angles α_H . The two panels show measurements acquired at symmetric angles around the FC direction. To clarify the evolution of the magnetization, the two branches of the experimental loops have been depicted with different filled symbols. The solid lines are the simulated curves obtained using the SW model with the anisotropy configurations depicted in Fig. 1 (a).

either always positive or negative) or in both semicircles (positive and negative), whereas for the collinear case M_{\perp} only reverses in one semicircle. Moreover, the angular range where M_{\perp} reverses in both semicircles is not symmetric around the FC direction. For instance, M_{\perp} reverses in both semicircles at $\alpha_H=-9^\circ$ whereas only in one at $\alpha_H=+9^\circ$. Additionally, the reversal asymmetry is not symmetric around the FC direction in the noncollinear case. Magnetization reversal via rotation processes is not always more relevant in the same field branch but can be found in either descending or ascending branches of the hysteresis loop, depending on the sign of the applied magnetic field angle with respect to the FC direction.

When comparing the angular dependence of the exchange bias and the coercivity, the symmetry breaking of the noncollinear coupling can be clearly observed (see Fig. 3). For example, $\mu_0 H_E=0$ is not found perpendicular to the FC direction, but at $\alpha_H=-81^\circ$ and $+99^\circ$. Both coercivity and exchange bias are not symmetric around the FC direction, i.e., $\mu_0 H_C(-\alpha_H) \neq \mu_0 H_C(+\alpha_H)$ and $\mu_0 H_E(-\alpha_H) \neq \mu_0 H_E(+\alpha_H)$. Around the FC direction, i.e., $\alpha_H=0^\circ$, the coercivity displays almost no variation which coincides with the occurrence of M_{\perp} reversal in both semicircles (see the area highlighted around 0° in Fig. 3). Additionally, the angular range where an asymmetric reversal behavior is observed is also not symmetric around the FC direction. In this case, we assign two critical angles at $\sim -25^\circ$ and $\sim +40^\circ$ to observe asymmetric magnetization reversal. Finally, these critical angles coincide with the onset of coercivity, i.e., $\mu_0 H_C \neq 0$, the onset of reversible processes, and the maximum exchange bias values found around the FC direction. In fact, the induced asymmetries can be exploited to tailor the magnetic behavior of FM/AFM systems, e.g., by significantly reducing $\mu_0 H_C$ while virtually keeping $\mu_0 H_E$ unchanged or having a biased 90° loop.

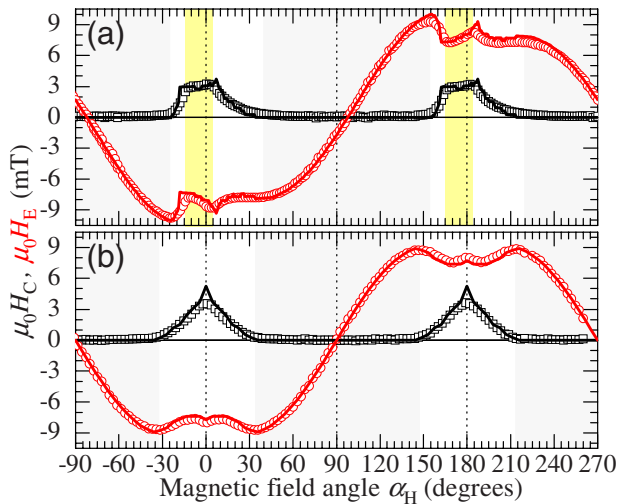


FIG. 3. (Color online) Angular dependence of exchange bias, $\mu_0 H_E$, and coercivity, $\mu_0 H_C$, for the (a) noncollinear and (b) collinear coupled Co/IrMn bilayer. The range of angles where only reversible processes take place during the reversal are marked by gray shadowed areas. The angular range around the FC direction where M_{\perp} reverses in both semicircles is also highlighted in light yellow. The symbols are the experimental values derived from Kerr measurements as those shown in Fig. 2. Continuous lines are the simulated curves obtained using the SW model with the anisotropy configurations depicted in Fig. 1(a).

All the nonsymmetric magnetic behaviors found experimentally in the noncollinear coupled FM/AFM bilayer are well reproduced without any fitting parameter with a simple coherent rotation Stoner-Wohlfarth model⁵ including K_U and K_E misaligned 20° , i.e., the FC angle with respect to the FM anisotropy direction, as shown the solid lines in the figures. Similar noncollinear configurations have already been used *ad hoc* to model recent experimental observations in exchange bias systems.^{6,12–15} In our case, the values K_U and K_E were extracted from the experimental data of the reference FM film and the FM/AFM bilayers. The same anisotropy values were used to simulate the behavior of bilayer with collinear anisotropies, i.e., $\beta_{FC}=0^\circ$, shown in Figs. 1 and 3.

In summary, the detailed angular dependence magnetic studies in exchange biased systems with collinear and noncollinear uniaxial and unidirectional anisotropies shows that a number of asymmetries can be induced by the noncollinearity [e.g., magnetization reversal, $\mu_0 H_E(-\alpha_H)$

$\neq \mu_0 H_E(+\alpha_H)$ and $\mu_0 H_C(-\alpha_H) \neq \mu_0 H_C(+\alpha_H)$]. This reveals the importance not only of the relative intensity of the different anisotropies in the system but also of the angle between them. The induced anisotropic behavior can be used to tailor the magnetic properties in exchange biased systems.

This work was supported in part by the Spanish MICINN through Project Nos. MAT2006-13470, MAT2007-66309-C02, HF2006-0197, and CSD2007-00010 and by the Comunidad de Madrid and the Generalitat de Catalunya through Project Nos. Nanomagnet S-0505/MAT/0194 and 2009-SGR-1292, respectively. Work at Argonne was supported by the UChicago Argonne, LLC through Contract No. DE-AC02-06CH1357.

¹W. H. Meiklejohn and C. P. Bean, *Phys. Rev.* **102**, 1413 (1956).

²See reviews, J. Nogués and I. K. Schuller, *J. Magn. Magn. Mater.* **192**, 203 (1999); A. E. Berkowitz and K. Takano, *ibid.* **200**, 552 (1999); R. L. Stamps, *J. Phys. D* **33**, R247 (2000); M. Kiwi, *J. Magn. Magn. Mater.* **234**, 584 (2001); F. Radu and H. Zabel, *Springer Tracts in Modern Physics* (Springer, Berlin, 2007), Vol. 227, pp. 97–184.

³H. Ohldag, A. Scholl, F. Nolting, E. Arenholz, S. Maat, A. T. Young, M. Carey, and J. Stöhr, *Phys. Rev. Lett.* **91**, 017203 (2003).

⁴J. Camarero, Y. Pennec, J. Vogel, S. Pizzini, M. Cartier, F. Fettar, F. Ernult, A. Tagliaferri, N. B. Brookes, and B. Dieny, *Phys. Rev. B* **67**, 020413(R) (2003).

⁵J. Camarero, J. Sort, A. Hoffmann, J. M. García-Martín, B. Dieny, R. Miranda, and J. Nogués, *Phys. Rev. Lett.* **95**, 057204 (2005).

⁶A. Tillmanns, S. Oertker, B. Beschoten, G. Güntherodt, J. Eisenmenger, and I. K. Schuller, *Phys. Rev. B* **78**, 012401 (2008).

⁷J. Nogués, D. Lederman, T. J. Moran, and I. K. Schuller, *Phys. Rev. Lett.* **76**, 4624 (1996).

⁸P. Miltényi, M. Gierlings, M. Bammig, U. May, G. Güntherodt, J. Nogués, M. Gruyters, C. Leighton, and I. K. Schuller, *Appl. Phys. Lett.* **75**, 2304 (1999).

⁹J. Nogués, T. J. Moran, D. Lederman, I. K. Schuller, and K. V. Rao, *Phys. Rev. B* **59**, 6984 (1999).

¹⁰J. Olamit, Z. P. Li, I. K. Schuller, and K. Liu, *Phys. Rev. B* **73**, 024413 (2006).

¹¹S. H. Chung, A. Hoffmann, and M. Grimsditch, *Phys. Rev. B* **71**, 214430 (2005).

¹²F. Radu, A. Westphalen, K. Theis-Bröhl, and H. Zabel, *J. Phys.: Condens. Matter* **18**, L29 (2006).

¹³M. J. M. Pires, R. B. de Oliveira, Jr., M. D. Martins, J. D. Ardisson, and W. A. A. Macedo, *J. Phys. Chem. Solids* **68**, 2398 (2007).

¹⁴J. McCord, C. Hamann, R. Schäfer, L. Schultz, and R. Mattheis, *Phys. Rev. B* **78**, 094419 (2008).

¹⁵E. Jiménez, J. Camarero, J. Sort, J. Nogués, A. Hoffmann, N. Mikuszeit, J. M. García-Martín, B. Dieny, and R. Miranda, *Phys. Rev. B* **80**, 014415 (2009).